Current-Induced Light Emission and Light-Induced Current in Molecular-Tunneling Junctions

Michael Galperin* and Abraham Nitzan
School of Chemistry, Tel Aviv University, Tel Aviv 69978, Israel
(Received 7 March 2005; published 8 November 2005)

The interaction of metal-molecule-metal junctions with light is considered within a simple generic model. We show, for the first time, that light-induced current in unbiased junctions can take place when the bridging molecule is characterized by a strong charge-transfer transition. The same model shows current-induced light emission under potential bias that exceeds the molecular excitation energy. Results based on realistic estimates of molecule-lead coupling and molecule-radiation field interaction suggest that both effects should be observable.

DOI: 10.1103/PhysRevLett.95.206802 PACS numbers: 73.23.−b, 78.20.Jq, 78.60.Fi, 78.67.−n

Molecular conduction nanojunctions have been under intense study for some time [1]. A class of molecules not yet investigated in this context are those characterized by strong charge-transfer transitions into their first excited state. The dipole moment of such molecules [2] changes considerably upon excitation, expressing a strong shift of the electronic charge distribution. In the independent electron picture this implies that either the highest occupied, or the lowest unoccupied, molecular orbitals (HOMO or LUMO) is dominated by atomic orbitals of larger amplitude (and better overlap with metal orbitals) on one side of the molecule than on the other and therefore stronger coupling to one of the leads. We show that when such molecular wire connects between two metal leads, optical pumping can create an internal driving force for charge flow between the leads. Such optical-resonance activation of current flow is different from previously demonstrated adiabatic pumping [3] and from previously discussed strong field optical control mechanisms [4,5]. The opposite phenomenon—light emission in current carrying tunnel junctions—has already been demonstrated. Emission from bare junction [6] was attributed to surface plasmons [7]. Emission from molecular nanojunctions [8,9] was discussed in Ref. [10].

Our model provides a simple unified framework for treating both light-induced current and current-induced light in molecular junctions. Following its introduction, we present numerical results and approximate expressions for the corresponding electron and photon fluxes. We examine, using experimentally based parameters, the magnitudes of these effects and conclude that both phenomena are observable under fairly general conditions.

In our model (see inset to Fig. 1) the molecule is represented by its HOMO, $|1\rangle$, and LUMO, $|2\rangle$, with energies ε_1 and ε_2 and gap $\varepsilon_{21} = \varepsilon_2 - \varepsilon_1$, positioned between two leads represented by free electron reservoirs $L(=\{|l\rangle\})$ and $R(=\{|r\rangle\})$ characterized by electrochemical potentials μ_L and μ_R. $\mu_L - \mu_R = e\Phi$ is the voltage bias. In the independent electron picture excitation transfers an electron between levels $|1\rangle$ and $|2\rangle$. The corresponding Hamiltonian is

$$\hat{H} = \hat{H}_0 + \hat{V}_M + \hat{V}_N + \hat{V}_P = \hat{H}_J + \hat{V}_N + \hat{V}_P, \quad (1)$$

$$\hat{H}_0 = \sum_{m=1,2} \varepsilon_m \hat{c}_m^\dagger \hat{c}_m + \sum_{k\in\{L,R\}} \varepsilon_k \hat{c}_k^\dagger \hat{c}_k + \hbar \sum_\alpha \omega_\alpha \hat{a}_\alpha^\dagger \hat{a}_\alpha, \quad (2)$$

$$\hat{V}_M = \sum_{K=L,R} \sum_{m=1,2;k\in K} (V_{km}^{(MK)} \hat{c}_k^\dagger \hat{c}_m + \text{H.c.}), \quad (3)$$

$$\hat{V}_N = \sum_{K=L,R} \sum_{k\neq k'\in K} (V_{kk'}^{(NK)} \hat{c}_k^\dagger \hat{c}_{k'} \hat{c}_2^\dagger \hat{c}_1 + \text{H.c.}), \quad (4)$$

$$\hat{V}_P = \begin{cases} (V_0^{(P)} \hat{a}_0 \hat{c}_2^\dagger \hat{c}_1 + \text{H.c.}) & \text{case } a \\ \sum_\alpha (V_\alpha^{(P)} \hat{a}_\alpha \hat{c}_2^\dagger \hat{c}_1 + \text{H.c.}) & \text{case } b \end{cases}, \quad (5)$$

where H.c. denotes Hermitian conjugate. $\hat{H}_0$ in (2) con-

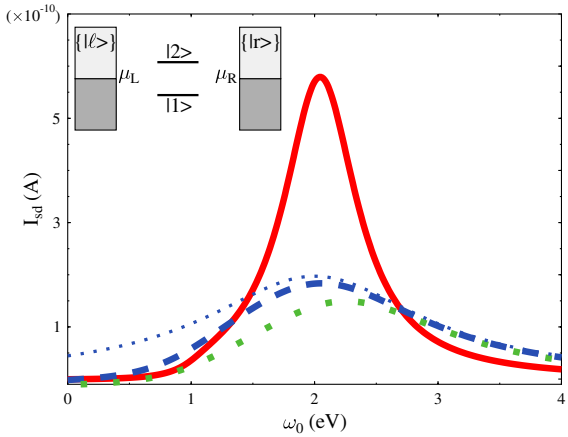

FIG. 1 (color online). The light-induced current in the model defined by Hamiltonian (1)–(5) and shown in the inset. Solid (red online) thick line: $T = 300$ K, $\varepsilon_{21} = 2$ eV, $\Gamma_{ML,1} = \Gamma_{MR,1} = 0.2$ eV, $\Gamma_{ML,2} = 0.02$ eV, $\Gamma_{MR,2} = 0.3$ eV, $\gamma_P = 10^{-6}$ eV, $B_{NL} = B_{NR} = 0.1$ eV, and $V_0^{(P)} = 10^{-3}$ eV. Dashed (blue online) thick line: same parameters as full line except $\Gamma_{MK,m} \times 3 (m = 1, 2)$ is used. Dashed-dotted (blue online) thin line: approximation (16) is used. Dotted (green online) thick line: same parameters as dashed line except $B_{NK} \times 10$ is used. The inset shows the molecular junction model (see text).

tains additive terms associated with the isolated molecule, the free leads, and the radiation field. Equations (3)–(5) describe the coupling between these subsystems. The operators $\hat{c}$ ($\hat{c}^\dagger$) and $\hat{a}$ ($\hat{a}^\dagger$) are annihilation (creation) operators for electrons and photons. $\hat{V}_M$ is the standard electron-transfer coupling that gives rise to net current in the biased junction and $\hat{V}_N$ describes energy transfer between the molecule and electron-hole excitations in the leads. The latter interaction strongly affects the lifetime of excited molecules near metal surfaces. The molecule-radiation field coupling $\hat{V}_P$, Eq. (5), will be taken in two forms: The form (5) (case *a*) describes driving of the junction by the electromagnetic field mode $\alpha = 0$; Eq. (5) (case *b*) is used to address spontaneous light emission from current carrying junctions. We limit ourselves to near resonance processes pertaining to linear spectroscopy. This justifies the rotating wave approximation (RWA) used in Eq. (5). Note that the radiative coupling coefficients reflect properties of the local electromagnetic field at the junction which depend on the metallic boundary conditions.

In the Keldysh nonequilibrium Green function approach [11] the steady state currents through the bridge are obtained from [12]

$$I_B = \int_{-\infty}^{+\infty} \frac{dE}{2\pi\hbar} \mathrm{Tr}[\mathbf{\Sigma}_\mathbf{B}^<(E)\mathbf{G}^>(E) - \mathbf{\Sigma}_\mathbf{B}^>(E)\mathbf{G}^<(E)] \quad (6)$$

where the Green functions (GFs) G and the self-energies (SEs) Σ are defined in the bridge subspace. The subscript B corresponds to a particular relaxation process represented by the SE $\Sigma_B^{\langle,\rangle}$. At steady state the absorption and emission photon fluxes I_{abs} and I_{em}, the nonradiative relaxation flux I_N, and the source-drain current I_{sd}, come into balance. The SEs needed for their evaluation are calculated as sums of independent contributions associated with the different relaxation processes (the noncrossing approximation)

$$\mathbf{\Sigma} = \mathbf{\Sigma_{ML}} + \mathbf{\Sigma_{MR}} + \mathbf{\Sigma_P} + \mathbf{\Sigma_{NL}} + \mathbf{\Sigma_{NR}} \quad (7)$$

where $\Sigma_X (X = ML, MR, P, NL, NR)$ is the SE associated with the coupling $V^{(X)}$ in Eqs. (3)–(5). On the Keldysh contour these SEs are 2×2 matrices in the bridge space

$$\Sigma_{MK,mm'}(\tau_1, \tau_2) = \sum_{k\in K} V_{mk}^{(MK)} g_k(\tau_1, \tau_2) V_{km'}^{(MK)}, \quad (8)$$

$$\Sigma_{NK,mm'}(\tau_1, \tau_2) = \delta_{mm'} \sum_{k\neq k'\in K} |V_{kk'}^{(NK)}|^2 g_k(\tau_2, \tau_1) g_{k'}(\tau_1, \tau_2) \times G_{\bar{m}\,\bar{m}}(\tau_1, \tau_2), \quad (9)$$

$$\mathbf{\Sigma}_\mathbf{P}(\tau_1, \tau_2) = i\sum_\alpha |V_\alpha^{(P)}|^2 \begin{bmatrix} F_\alpha(\tau_2, \tau_1) G_{22}(\tau_1, \tau_2) & 0 \\ 0 & F_\alpha(\tau_1, \tau_2) G_{11}(\tau_1, \tau_2) \end{bmatrix}; \quad (10)$$

here and below $K = L, R$ denotes the left and right leads, $m, m' = 1, 2$ and $\bar{m} = 2\delta_{m,1} + \delta_{m,2}$. g_k and F_α are free electron and photon GFs in state k and mode α, respectively. The retarded or advanced, lesser and greater projections of these SEs on the real time axis are obtained using the Langreth formulas [11] and can be expressed at steady state situations in energy space. In the wide-band approximation and assuming that the HOMO and LUMO are not mixed by their interactions with the leads, the SEs associated with electron exchange between molecule and leads have the familiar forms $\Sigma^r_{MK,mm'} = [\Sigma^a_{MK,m'm}]^* = -i\delta_{mm'}\Gamma_{MK,m}/2$, $\Sigma^<_{MK,mm'} = i\delta_{mm'} f_K(E)\Gamma_{MK,m}$, $\Sigma^>_{MK,mm'} = -i\delta_{mm'}[1 - f_K(E)]\Gamma_{MK,m}$ where $\Gamma_{MK,m} = 2\pi\sum_{k\in K}|V_{km}^{(MK)}|^2\delta(E - \varepsilon_k)$ and $f_K(E) = [\exp\{(E - \mu_K)/k_BT\} + 1]^{-1}$. The SEs associated with the nonradiative and radiative energy relaxation processes are similarly obtained in the forms $\Sigma^<_{NK,mm'}(E) = \delta_{mm'}\int\frac{d\omega}{2\pi} B_{NK}(\omega, \mu_K) G^<_{\bar{m}\,\bar{m}}(E + \omega)$, $\Sigma^>_{NK,mm'}(E) = \delta_{mm'}\int\frac{d\omega}{2\pi} B_{NK}(\omega, \mu_K) G^>_{\bar{m}\,\bar{m}}(E - \omega)$, where

$$B_{NK}(\omega, \mu_K) = 2\pi \sum_{\substack{k,k'\in K \\ k\neq k'}} |V_{kk'}^{(NK)}|^2 \delta(\varepsilon_k + \omega - \varepsilon_{k'}) f_K(\varepsilon_k) \times [1 - f_K(\varepsilon_{k'})] \quad (11)$$

and

$$\mathbf{\Sigma}^<_\mathbf{P}(E) = \sum_\alpha |V_\alpha^{(P)}|^2 \begin{bmatrix} (1 + N_\alpha) G^<_{22}(E + \omega_\alpha) & 0 \\ 0 & N_\alpha G^<_{11}(E - \omega_\alpha) \end{bmatrix}, \quad (12a)$$

$$\mathbf{\Sigma}^>_\mathbf{P}(E) = \sum_\alpha |V_\alpha^{(P)}|^2 \begin{bmatrix} N_\alpha G^>_{22}(E + \omega_\alpha) & 0 \\ 0 & (1 + N_\alpha) G^>_{11}(E - \omega_\alpha) \end{bmatrix}, \quad (12b)$$

where N_α is the number of photons in mode α. The corresponding retarded and advanced SEs are more difficult to calculate from the Langreth rules. For simplicity we assume, in the spirit of the wide-band approximation, that all diagonal components of Σ are purely imaginary. Consequently

$$\mathbf{\Sigma}^\mathbf{r}(E) = [\mathbf{\Sigma}^\mathbf{a}(E)]^\dagger = \frac{[\mathbf{\Sigma}^>(E) - \mathbf{\Sigma}^<(E)]}{2} \equiv -\frac{i}{2}\mathbf{\Gamma}. \quad (13)$$

We use (13) to get the retarded and advanced GFs according to $G^r_{mm'}(E) = (G^a_{m'm}(E))^* = [E - \varepsilon_m - \Sigma^r_{mm}(E)]^{-1} \times \delta_{mm'}$. $G^{\langle,\rangle}$ needed in (6) are then obtained from the Keldysh equation $\mathbf{G}^{\langle,\rangle}(E) = \mathbf{G}^\mathbf{r}(E)\mathbf{\Sigma}^{\langle,\rangle}(E)\mathbf{G}^\mathbf{a}(E)$. After evaluating these matrices we can use Eq. (6) with the appropriate self-energy terms to calculate the desired flux. We are particularly interested in I_{em} and I_{sd}.

With regard to the radiative interactions we consider two models: (A) To study the effect of pumping the junction

with light we use a model with a single photon mode of frequency ω_0, as described by Eq. (5) (case *a*). In the semiclassical limit for the radiation field and in the RWA we can set $N_0 = 1$ and take the coupling $\hat{V}_0^{(P)}$ as a product of the local electric field amplitude and the molecular transition dipole. The charge-transfer transition on the bridge is expressed in this model by taking LUMO bridge level more strongly coupled to one lead than to the other. For the HOMO this inequality is assumed weaker or reversed. The flux of interest is $I_{\rm sd}$ under illumination. (B) To describe current driven spontaneous emission we use the interaction (5) (case *b*) with all radiation field modes taken in their vacuum state. The frequency resolved emission, $I'_{\rm em}(\omega) = dI_{\rm em}(\omega)/d\omega$ is obtained from (6) using the frequency resolved self-energies obtained from (12)

$$\mathbf{\Sigma}_{\mathbf{P}}^{<}(E,\omega) = \frac{\gamma_P(\omega)}{2\pi\rho_P(\omega)}\begin{bmatrix} G_{22}^{<}(E+\omega) & 0 \\ 0 & 0 \end{bmatrix}, \tag{14a}$$

$$\mathbf{\Sigma}_{\mathbf{P}}^{>}(E,\omega) = \frac{\gamma_P(\omega)}{2\pi\rho_P(\omega)}\begin{bmatrix} 0 & 0 \\ 0 & G_{11}^{>}(E-\omega) \end{bmatrix}, \tag{14b}$$

with the radiative width $\gamma_P(\omega) = 2\pi|V_\alpha^{(P)}|_\omega^2\rho_P(\omega)$ and the density of photon modes, $\rho_P(\omega) = \omega^2/(\pi^2c^3)$ where c is the speed of light. The total emission flux is found from $I_{\rm em}^{\rm tot} = \int_0^\infty d\omega I'_{\rm em}(\omega)$.

In general, the coupled equations for the self-energies and the Green functions have to be solved self-consistently. The numerical results displayed below were obtained from such an iterative solution under the wide-band approximation. More transparent closed forms may be written under the additional simplifying assumptions: (a) ε_{21} is large relative to the total widths of levels 1 and 2; (b) keep only the lowest (second) order in the radiative coupling $\hat{V}_P$. It is then possible to express the relevant self-energies and the resulting currents in terms of the electronic populations n_1 and n_2 of levels 1 and 2 using $n_m = (2\pi i)^{-1}\int_{-\infty}^{+\infty} dE G_{mm}^{<}(E)$, $m = 1, 2$. In addition, for case (A) we are interested in the small or no voltage regime, whereupon to a good approximation $n_1 = 1$ and $n_2 = 0$. This leads, for model (A), to [13]

$$I_{\rm sd} = \int \frac{dE}{2\pi\hbar}\sum_{m=1,2}\Gamma_{ML,m}G_{mm}^r(E)\Gamma_{MR,m}G_{mm}^a(E)[f_L(E) - f_R(E)] + |V_0^{(P)}|^2\int\frac{dE}{2\pi\hbar} \times \frac{\Gamma_{ML,1}\Gamma_{MR,2}f_L(E-\omega_0)[1-f_R(E)] - \Gamma_{ML,2}\Gamma_{MR,1}f_R(E-\omega_0)[1-f_L(E)]}{[(E-\varepsilon_2)^2 + (\Gamma_2/2)^2][(E-\omega_0-\varepsilon_1)^2 + (\Gamma_1/2)^2]}. \tag{15}$$

The first term on the right is the usual Landauer term that vanishes at zero bias, $f_L = f_R$. The second term shows explicitly the effect of illumination. In the absence of bias, $f_L = f_R \equiv f$, and for $\omega_0 \approx \varepsilon_{21}$, Eq. (15) is dominated by $E \approx \varepsilon_2$ so we may approximate $f(E-\omega_0)[1-f(E)] \sim 1$. This leads to

$$I_{\rm sd} = \frac{|V_0^{(P)}|^2}{\hbar}\frac{\Gamma}{(\varepsilon_2 - \omega_0 - \varepsilon_1)^2 + (\Gamma/2)^2}\frac{\Gamma_{ML,1}\Gamma_{MR,2} - \Gamma_{ML,2}\Gamma_{MR,1}}{\Gamma_1\Gamma_2}. \tag{16}$$

Equation (16) shows explicitly how asymmetry in the HOMO and LUMO couplings to the metal electrodes leads to photocurrent in the present model. This asymmetry, which reflects the charge-transfer character of the HOMO → LUMO transition, creates a molecular photovoltage that drives this current.

For model (B) the frequency resolved emission is obtained from (6) and (14) in the form

$$I'_{\rm em}(\omega) = \frac{\gamma_P(\omega)}{\hbar}\int_{-\infty}^{+\infty}\frac{dE}{2\pi}\left\{\frac{f_L(E+\omega)\Gamma_{ML,2} + f_R(E+\omega)\Gamma_{MR,2}}{(E+\omega-\varepsilon_2)^2 + (\Gamma_2/2)^2}\frac{[1-f_L(E)]\Gamma_{ML,1} + [1-f_R(E)]\Gamma_{MR,1}}{(E-\varepsilon_1)^2 + (\Gamma_1/2)^2}\right\} \tag{17}$$

and the integrated emission is obtained, using the same approximations as before, in the anticipated form [13]

$$I_{\rm em}^{\rm tot} = \frac{\gamma_P(\varepsilon_{21})}{\hbar}n_2(1-n_1). \tag{18}$$

The level populations n_1 and n_2 should be obtained from the full self-consistent calculation. For $\Phi > \varepsilon_{21}$ both LUMO and HOMO bridge levels are well inside the energy window between the leads' chemical potentials. A good approximation for these populations is (written for the case of negatively biased left electrode) $n_2 = \Gamma_{ML,2}/\Gamma_2$; $n_1 = \Gamma_{ML,1}/\Gamma_1 + n_2(B_N + \gamma_P)/\Gamma_1$. Equation (18) then leads to

$$I_{\rm em}^{\rm tot} = \frac{\gamma_P}{\hbar}\frac{\Gamma_{ML,2}\Gamma_{MR,1}}{\Gamma_1\Gamma_2}. \tag{19}$$

Comparing to (16) we see that tailoring the molecule-leads coupling asymmetry such that resonance radiation will induce electron flow in a given direction enhances light emission under such bias that leads to electron current in the opposite direction.

Numerical results obtained from Eqs. (15) and (17) and the self-consistent calculation are shown in Figs. 1 and 2. Figure 1 shows the light-induced current obtained using reasonable junction parameters. In particular, for a molecule with transition dipole moment ~1D the choice $V_0^{(P)} = 10^{-3}$ eV corresponds to a local field intensity

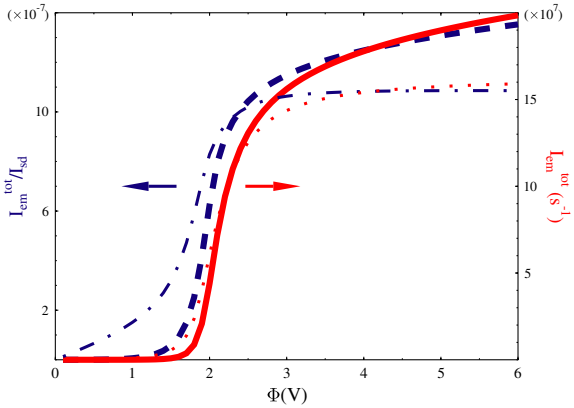

FIG. 2 (color online). The integrated photon emission rate (solid thick line, red online) and yield (dashed thick line, blue online) plotted against the bias voltage. Parameters are as in the solid line of Fig. 1 except $\Gamma_{MK,m} = 0.1$ eV, $K = L, R$, $m = 1, 2$. The thin dotted and dashed-dotted lines are results for the integrated emission and yield, respectively, based on the approximation (18).

$\sim 10^8$ watt/cm^2. The analytical approximation (16) also works well for this choice of parameters. Note that increasing the electron-transfer coupling Γ broadens the response feature, as expected, however the sensitivity to the energy transfer coupling B is much weaker as long as the level energetics is such that the HOMO level is fully occupied while the LUMO is fully empty [13]. It is seen only for larger Γ, where the broadened molecular levels start to overlap the Fermi energy (compare the dashed and the thick dotted lines in Fig. 1). In this case also the quality of the approximation (16) deteriorates, as shown.

Figure 2 shows the integrated emission (solid line) and the predicted photon emission yield (the integrated emission flux divided by the electronic current passed by the junction, dashed line) plotted against the bias voltage. Also shown are the corresponding results based on the approximation (18). This approximation, which neglects level broadening, improves for smaller Γ_{MK}.

These results, obtained under rather conservative choices of damping parameters, indicate that both light-induced current and the molecular mechanism (as opposed to the surface plasmon mechanism) for current-induced emission in tunnel junctions can lead to measurable signals. This molecular mechanism can, in principle, be distinguished from the plasmon mechanism for light emission by the frequency dependence of the resolved emission, as implied by Eq. (17).

In conclusion, we have described a model that accounts for observed current-induced light emission from molecular tunnel junctions and provides the tools for determining the intensity and yield of such emission as functions of key junction parameters. The same model predicts that resonant light-induced current can occur in junctions employing molecular bridges with strong charge-transfer transition to their first excited state. We have found, using reasonable parameters, that light driven electronic currents and current driven light emission are realistic possibilities. The linewidths and line shapes associated with these signals can also be analyzed by the same theoretical framework. Correlating observations with predictions made in this Letter should help the interpretation of future experiments in this direction, and may add a valuable tool for monitoring the molecular component in molecular conduction junctions. Finally, the inclusion of the energy transfer interaction (4) is a new element not previously considered in the theory of molecular junctions [14]. Interestingly its effect in reducing the yield of the phenomena discussed above is found to be small. Its role in other situations pertaining to the operation of molecular junctions will be addresses elsewhere.

We acknowledge support from the Israel Science Foundation, the US-Israel BSF, and by the NSF/NCN project through Northwestern University. We thank Professor T. Marks and Professor M. Ratner for helpful discussions and support.

*Present address: Department of Chemistry, Northwestern University, Evanston IL 60208, USA.

[1] See, e.g., Issue on Molecular Transport Junctions, edited by C. R. Kagan and M. A. Ratner [MRS Bull. **29**, 376 (2004)]; Molecular Electronics Special Feature, edited by C. Joachim and M. A. Ratner [Proc. Natl. Acad. Sci. U.S.A. **102**, 8800 (2005)].
[2] See, e.g., S. N. Smirnov and C. L. Braun, Rev. Sci. Instrum. **69**, 2875 (1998).
[3] M. Switkes *et al.*, Science **283**, 1905 (1999).
[4] J. Lehmann *et al.*, Chem. Phys. Lett. **368**, 282 (2003).
[5] M. Moskalets and M. Buttiker, Phys. Rev. B **69**, 205316 (2004).
[6] J. K. Gimzewski *et al.*, Z. Phys. B **72**, 497 (1988).
[7] B. Persson and A. Baratoff, Phys. Rev. Lett. **68**, 3224 (1992).
[8] E. Flaxer, O. Sneh, and O. Cheshnovsky, Science **262**, 2012 (1993).
[9] X. H. Qiu, G. V. Nazin, and W. Ho, Science **299**, 542 (2003).
[10] J. Buker and G. Kirczenow, Phys. Rev. B **66**, 245306 (2002).
[11] See, e.g., H. Haug and A.-P. Jauho, *Quantum Kinetics in Transport and Optics of Semiconductors* (Springer, Berlin, 1996).
[12] Y. Meir and N. S. Wingreen, Phys. Rev. Lett. **68**, 2512 (1992).
[13] M. Galperin and A. Nitzan (to be published).
[14] See, e.g., S. Datta, *Quantum Transport: Atom to Transistor* (Cambridge University Press, Cambridge, 2005).